

2nd CIRP Conference on Composite Material Parts Manufacturing (CIRP-CCMPM 2019)

# In Situ Joining of Unidirectional Tapes on Long Fiber Reinforced Thermoplastic Structures by Thermoplastic Automated Fiber Placement for Scientific Sounding Rocket Applications

Ralf Engelhardt<sup>a,\*</sup>, Stefan Ehard<sup>b</sup>, Tobias Wolf<sup>a</sup>, Jonathan Oelhafen<sup>c</sup>, Andreas Kollmannsberger<sup>a</sup>, Klaus Drechsler<sup>a</sup>

<sup>a</sup>Technical University of Munich, TUM Department of Aerospace and Geodesy, Chair of Carbon Composites, Boltzmannstr. 15, 85748 Garching, Germany

<sup>b</sup>Airbus Defence and Space GmbH, Rechliner Str., 85077 Manching, Germany

<sup>c</sup>fos4X GmbH, Thalkirchner Str. 210, 81371 Munich, Germany

\* Corresponding author. Tel.: +49-89-28910314; E-mail address: [ralf.engelhardt@tum.de](mailto:ralf.engelhardt@tum.de)

## Abstract

Automated Fiber Placement allows the automated lay-up of tailored laminates in aerospace quality. For thermoplastic matrix materials, the use of closed-loop temperature control enables an in situ consolidation. This makes autoclave curing superfluous and increases the overall process efficiency. Scientific sounding rockets typically consist of several aluminum modules carrying the scientific payload. The design of a module includes a cylindrical outer shell and two load input rings with a defined assembly interface. Reducing the structural weight would allow higher payloads, higher apogees or reduced fuel consumption. A new manufacturing concept using the Thermoplastic Automated Fiber Placement (TP-AFP) process was developed to manufacture a lightweight composite module.

This paper presents the developed concept and focuses on the characterization of an in situ joint of TP-AFP tapes on a long fiber reinforced thermoplastic (LFT) structure. This represents the joint of the cylindrical shell on the load input rings of the rocket module. The joint was characterized with single lap shear tests for two different sample extraction areas at room temperature and at elevated temperature on pre-treated and untreated LFT surface.

The variations did not show significant effects on the resulting shear strength. The results were considered for the design of the composite module allowing a weight reduction of more than 40 % compared to the aluminum modules. The new module proved its airworthiness as part of the sounding rocket mission REXUS-23 in March 2019. Beyond sounding rockets, the concept of in situ bonded TP-AFP tapes on complex LFT structures has many potential applications within aerospace but also automotive structures.

© 2020 The Authors. Published by Elsevier B.V.

This is an open access article under the CC BY-NC-ND license (<http://creativecommons.org/licenses/by-nc-nd/4.0/>)

Peer-review under responsibility of the scientific committee of the 2nd CIRP Conference on Composite Material Parts Manufacturing.

**Keywords:** Automated Fiber Placement; Thermoplastic composites; In situ consolidation; Sounding rockets;

## 1. Introduction

The production of structural aerospace components requires the combination of curved shells with complex stiffening or load introduction components. Fuselage and wing shells in stressed skin design together with frames and spars are typical examples. The connection of the different structures is typically realized by mechanical fasteners such as rivets [1,2]. For composite materials, adhesive bonding or – in case of

thermoplastic matrix material – fusion bonding are promising alternatives [3]. However, these approaches require several process steps and add additional materials to the structure.

Thermoplastic Automated Fiber Placement (TP-AFP) allows load path oriented lay-up of carbon fiber reinforced polymer (CFRP) shell structures with a high degree of automation. Labor-intensive steps can be reduced and a constant laminate quality can be guaranteed and monitored. In addition, thermoplastic composites offer several advantages

due to their long shelf life and recyclability. In situ consolidation of thermoplastic composites opens the possibility to reduce processing time and costs compared to a thermoset autoclave cure cycle. In situ joints between structures of the same material system reduce the amount of separate materials and increase the structure's potential for recycling. [4–7]

Press-forming or compression molding of long fiber reinforced thermoplastic (LFT) material can be used for the manufacturing of complex monolithic structures subjected to complex load cases. [8–10]

An application example and the motivation of the presented work is the development and implementation of a manufacturing concept for the thermoplastic composite module of a scientific sounding rocket. The concept comprises separate manufacturing processes of the thick, monolithic load input rings and the cylindrical shell. The rings are manufactured by LFT-press-forming, the shell structure by TP-AFP (cf. Fig. 1). [11]

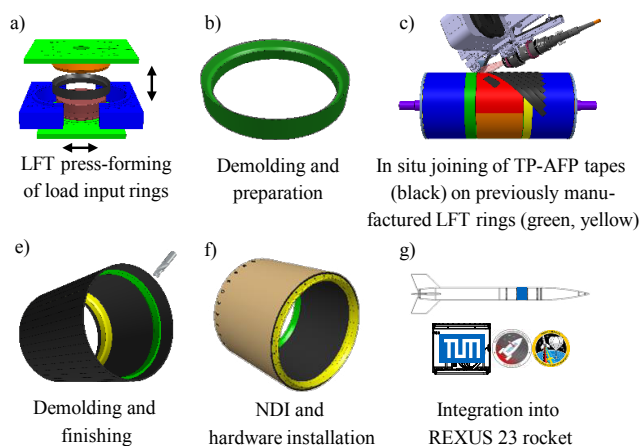


Fig. 1. Manufacturing concept for a thermoplastic CFRP module for a scientific sounding rocket [10].

This paper describes the characterization of the in situ joint of TP-AFP tapes on an LFT structure by single lap shear trials at room and service temperature. This represents the connection of the LFT load input rings and the cylindrical TP-AFP shell of the described rocket module (cf. Fig. 1 c).

## 2. Materials and methods

### 2.1. Equipment

The fiber placement was realized with a TP-AFP machine by AFPT GmbH (Dörth, Germany). The robot-guided placement head feeds thermoplastic CFRP tape towards the fusion zone. A 4 kW diode laser with near infrared wavelength is used to heat both joining partners, tape and substrate material (cf. Fig. 2). A closed-loop control system regulates the laser power and laser spot orientation to maintain the set temperature in the fusion zone. Incoming tape and substrate are heated above melting temperature and bonded under pressure by a silicone roller. The fast and precise control of the process

temperature allows a so-called in situ consolidation without the need of subsequent consolidation steps. [12]

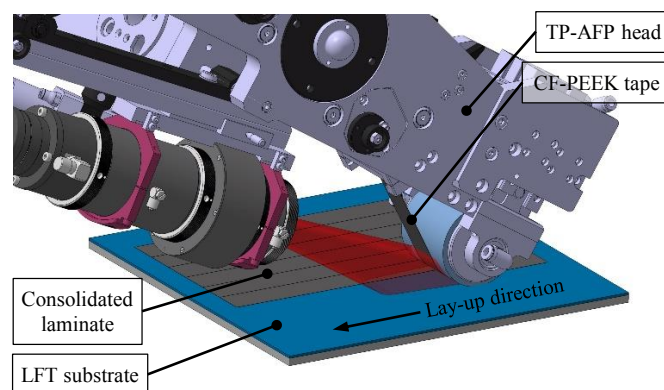


Fig. 2. TP-AFP process principle for joining TP tapes on LFT substrate [4].

The TP-AFP process parameters used in this study are based on pre-trials including a parameter optimization. The effective consolidation pressure based on the machine settings of the pneumatic roller actuator including the mean contact areas was evaluated in separate studies [13,14]. Samples with varying nip-point temperature, lay-up velocity and consolidation pressure were manufactured and evaluated with wedge peel tests. The resulting optimum parameter set is summarized in Table 1.

Table 1. TP-AFP process parameters.

		Ply 1	Ply 2-7
Nip point temperature	[°C]	485	485
Lay-up velocity	[m/min]	6.0	6.0
Consolidation pressure	[MPa]	0.34	0.46

An LFT plate of 300 x 300 x 3 mm was manufactured. It was press-formed using a heated two-sided tool compacted by vacuum. It was heated in the heat bed of a thermoforming press by Rucks Maschinenbau GmbH (Glauchau, Germany) to a processing temperature of 400 °C for a dwell time of 300 s with a heat and cool rate of 15 K/min.

### 2.2. Material

The material system for the TP-AFP process used in this study was the carbon fiber reinforced polyether ether ketone (PEEK) tape Tenax®-E TPUD PEEK-HTS45. It has a width of 25.4 mm, a matrix content of 34 wt% and a nominal thickness of 0.14 mm. [15]

For the press-forming process, the carbon fiber reinforced PEEK granules Victrex® 450CA30 with a fiber volume content of 30 % were used [16].

### 2.3. Experimental set-up

The performed test is based on the test standard ASTM D5868 [17] describing a method to characterize the joint between two fiber reinforced polymer structures. The

specimen geometry was adapted to the requirements of the used material combination and their in situ joint as shown in Fig. 3 and further described in section 2.4. A universal testing machine by Hegewald & Peschke Meß- und Prüftechnik GmbH (Nossen, Germany) with a maximum force of 250 kN and a heat chamber for tests at elevated temperatures was used. Fig. 3 shows the specimen geometry with aluminum spacers at the ends to avoid a tilted clamping. Tests were performed at room temperature and at 135 °C, as this is the maximum service temperature defined in the specifications of the scientific sounding rocket program.

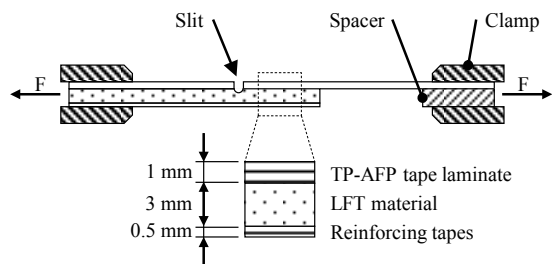


Fig. 3. Sample geometry adapted from ASTM D5868.

The shear strength of the overlap is calculated as follows:

$$T = \frac{F_{max}}{A} \quad (1)$$

with  $A$  being the overlap area of the joint and  $F_{max}$  the maximum force measured.

#### 2.4. Manufacturing of the samples

Seven unidirectional (UD) layers of TP-AFP tape were placed on the LFT plate. The low tensile strength of the LFT material leads to the risk of a failure not at the joint but within the LFT structure. To avoid this, the LFT structure was reinforced in advance with four layers of TP-AFP tape on the backside as depicted in Fig. 4 and Fig. 5. Three 0° layers along the testing direction were added and backed with one 90° layer to avoid bending due to asymmetric lay-up.

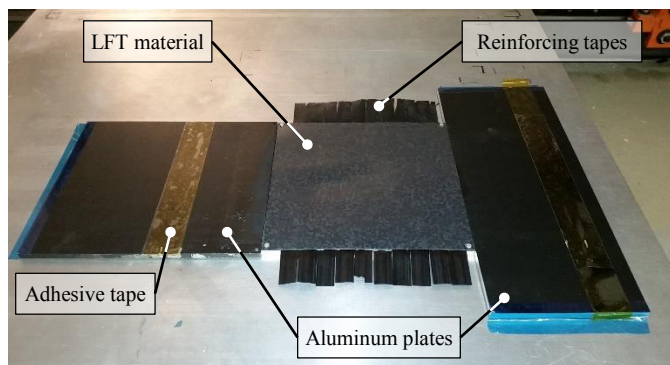


Fig. 4. Set-up of the LFT plate in the TP-AFP cell before lay-up of the seven layers on top of the LFT plate.

The reinforced LFT plate was mounted in the TP-AFP cell as shown in Fig. 4. Aluminum plates around the LFT structure created a levelled working surface.

Black temperature-resistant paint avoided unwanted reflections of the laser beam during lay-up of the first ply. Double-sided temperature-resistant adhesive tape supported the lay-up of the first ply.

This set-up allows a sample extraction in two different areas as shown in Fig. 5. The joint quality at the beginning of the LFT structure may differ from the rest as the closed-loop control has a certain response time for sudden changes of the substrate characteristics. The specimen area at the end of the LFT structure represents a joint with stabilized control parameters.

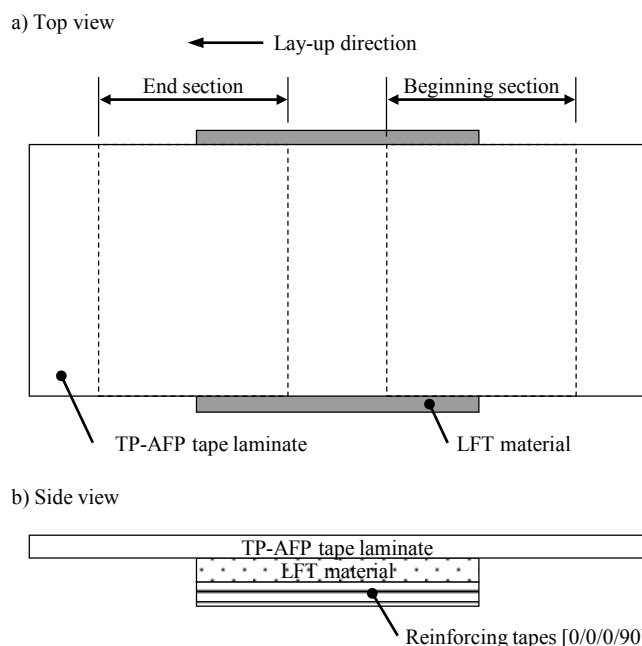


Fig. 5. Sample design and extraction areas.

In addition, the influence of mechanical surface treatment was to be investigated, as this corresponds to the machined surface of the LFT structure in the later rocket application.. Half of the LFT structure was left untreated. The other half was grinded with grit 80 sand paper. The described parameter variations led to the specimen set and nomenclature shown in Fig. 6. Each combination was tested with at least four samples. The samples were slitted as shown in Fig. 3 to apply the force to the joint surface.

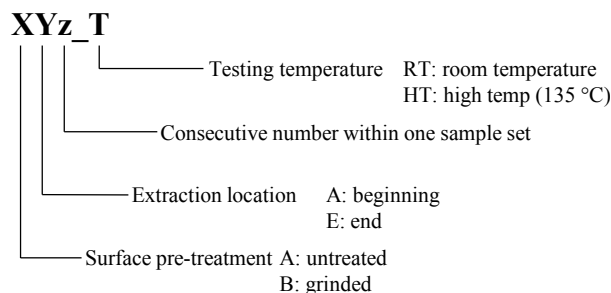


Fig. 6. Sample variations and nomenclature.

2.5. Experimental procedure

After cutting and measuring each sample, they were adjusted and fixed with a free clamping length of 112.5 mm in the clamps inside the thermal chamber of the universal testing machine (cf. Fig. 7). The test temperature was monitored by a thermocouple (TC) on the sample. The tests were executed with a speed of 1 mm/min.

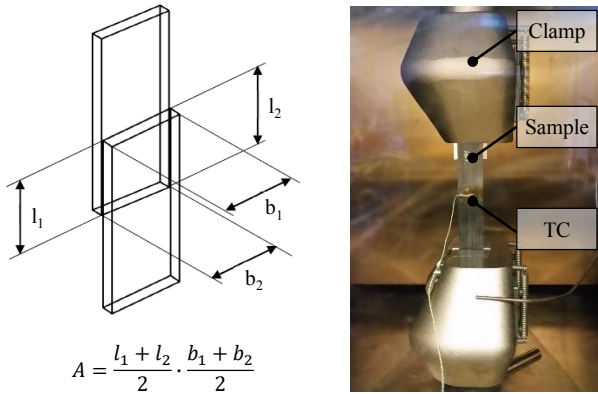


Fig. 7. Sample joint measuring and set-up in the thermal chamber of the testing machine.

3. Results and discussion

3.1. Result overview

Not all samples failed as intended, but showed other failure modes (cf. Fig. 8). The sample combinations AA\_RT and AE\_RT mostly fail within the joint. BA\_RT and AE\_HT also fail in the joint or slightly below the joint area. The sample combinations AA\_HT and BA\_HT mostly fail below the joint inside the LFT material. An exception is sample combination BE\_RT where the failure appears inside the TP-AFP tape.

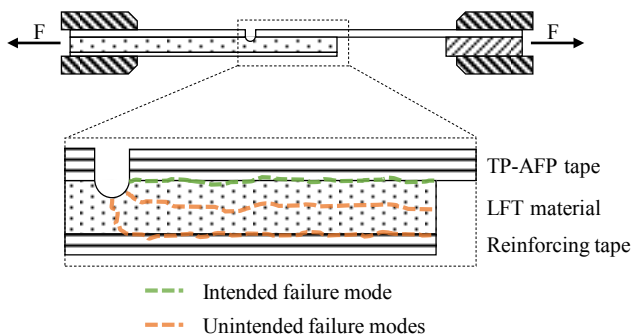


Fig. 8. Failure modes for the given experimental set-up.

The high temperature samples show a different behavior compared to the room temperature samples. While the room temperature samples mostly fail abruptly, the high temperature samples form a plateau before failure. It can be observed that the HT samples mostly fail at higher displacements compared to the RT samples. In Fig. 9, all samples are plotted with their maximum force at the corresponding displacement.

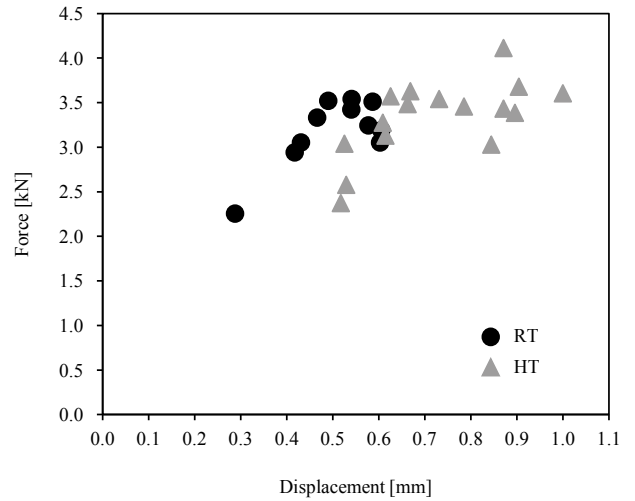


Fig. 9. Force displacement overview for all samples.

The HT samples show a significantly higher elongation at break due to the “softening” of the matrix around  $T_g$  (see also Fig. 12).

Fig. 10 summarizes the calculated shear strength of the sample combinations. Samples with an incorrect fracture plane were excluded.

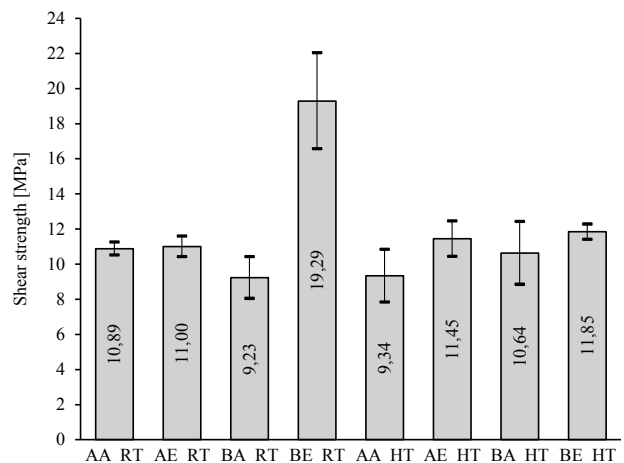


Fig. 10. Calculated shear strength for all sample variations.

3.2. Discussion

The results in Fig. 10 show significantly higher shear strengths for the samples BE\_RT compared to the rest. The reason for this turned out to be an inaccurate preparation of these samples. The milled slot that separates the TP-AFP tapes was not deep enough (cf. Fig. 11 middle).



Fig. 11. Tape failure (left), incorrect slit depth (middle), correct slit (right).

The remaining carbon fibers are bearing load under tension and fail at the transition to the LFT material due to stress peaks.

The differences between the RT and HT samples can be explained by the temperature dependent properties of semi-crystalline thermoplastic polymers [18]. The test temperature of 135 °C is just below the glass transition temperature  $T_g$  of PEEK of 143 °C [15,16]. Fig. 12 shows the qualitative thermal behavior of semi-crystalline thermoplastics. The storage modulus shows a drop around the  $T_g$ . This behavior is referred to as "softening" of the polymer near  $T_g$ . It reduces the peak stresses at the edges of the joint and therefore can increase  $F_{max}$ . [18,19]

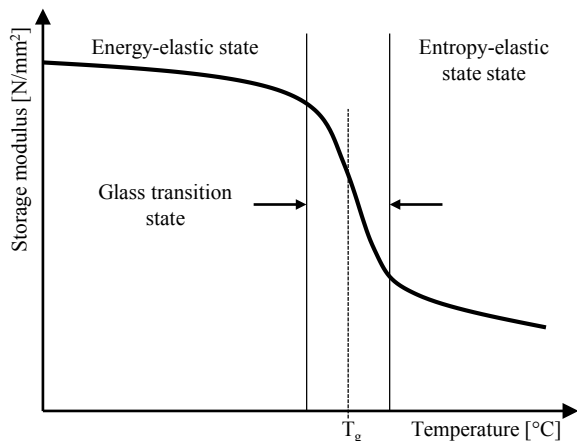


Fig. 12. Temperature dependent storage modulus of semi-crystalline thermoplastic polymers (based on [4]).

Fig. 10 shows that the shear strength values of the samples from the end of the LFT plate are slightly higher compared to the samples taken from the beginning. This can be explained by the increasing stabilization of the process. However, considering the standard deviation, the differences are not significant.

The samples with pre-treated surface show at room temperature slightly lower and at high temperature, slightly higher shear strengths compared to the unprepared surface samples. Considering the standard deviation, these differences are again not significant.

A microscope analysis of samples of the different settings shows no visual difference in the quality of the bond. No porosity or blisters are visible. Fig. 13 shows an exemplary microsection of a BE-sample.

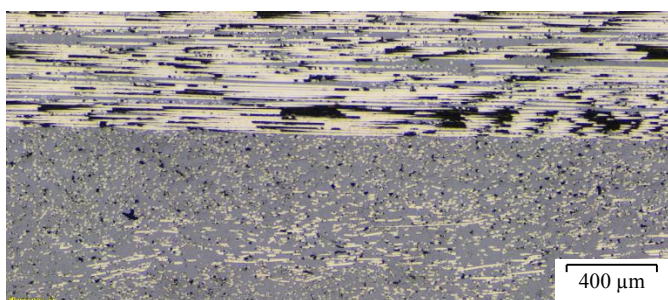


Fig. 13. Microsection of an untested in situ joint of TP-AFP tape (top) on LFT material (bottom).

The application of single lap shear tests for the given scenario has to be considered with care. The geometric asymmetry and uneven stiffness of the material combination causes a bending moment in addition to the tensile force. The joint is subjected to unintended peel stress in addition to shear stress. The comparability of the absolute values to the results of other set-ups might therefore lead to wrong assumptions, but a relative comparison within one set-up as presented in this study is valid. [13]

#### 4. Conclusion

The tests performed in this study characterize the in situ joint of TP-AFP tapes on an LFT structure. This represents the joint of the TP-AFP shell on LFT load input rings of a scientific sounding rocket module. Pre-trials with wedge peel samples defined the TP-AFP process parameters for the first ply and the subsequent laminate.

Single lap shear tests were used to characterize the joint for untreated and pre-treated surface, at room temperature and elevated temperature (135 °C) and for two different areas regarding the lay-up direction. The area at the beginning represents the application scenario of joining the TP-AFP shell structure of the sounding rocket module on the short LFT load input rings. The area at the end represents a manufacturing with stabilized process conditions for longer joints. For a treated surface, the average shear strength at room temperature is  $9.23 \text{ MPa} \pm 1.19 \text{ MPa}$  and at 135 °C  $11.24 \text{ MPa} \pm 1.43 \text{ MPa}$ . For an untreated surface,  $10.94 \text{ MPa} \pm 0.49 \text{ MPa}$  is achieved at room temperature and  $10.66 \text{ MPa} \pm 1.55 \text{ MPa}$  at high temperature. The comparison between RT and HT shows minor differences that cannot be considered significant considering the standard deviations. At higher temperatures, the shear strengths tend to be higher. Due to the softening of the thermoplastic matrix near the glass transition temperature, failure at high temperatures generally occurs later. The single lap shear specimens from the end of the LFT material provide slightly higher shear strength values than the specimens from the beginning due to a stabilized lay-up process.

The results of the characterization were considered as input for the design of the scientific sounding rocket module. The module was built, tested and qualified for flight [11,20].

It was launched in the research mission "REXUS" of the German Aerospace Center (DLR), Swedish National Space Agency (SNSA) and European Space Agency (ESA) on 4<sup>th</sup> of March 2019 as part of rocket REXUS 23 to an apogee of 75,42 km (cf. Fig. 14) [21]. It was the first in situ consolidated structure of its kind able to show its airworthiness in an actual flight.

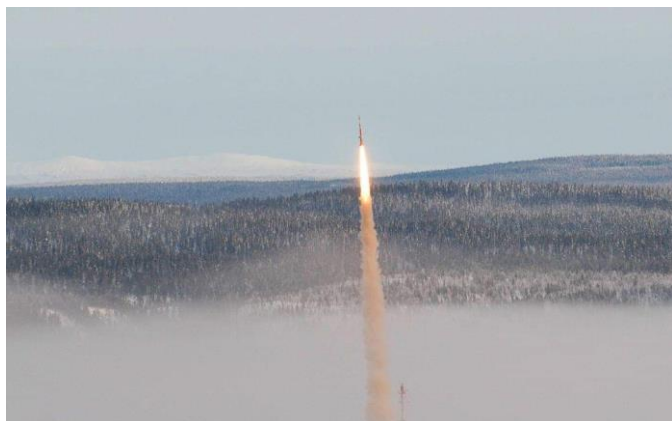


Fig. 14. Launch of REXUS 23 in Esrange (Sweden) on 4<sup>th</sup> of March 2019.

Beyond scientific sounding rockets, the concept of in situ bonded TP-AFP tapes on complex monolithic LFT structures has many potential applications within aerospace but also automotive structures.

### Acknowledgements

The authors would like to thank the German Federal Ministry for Economic Affairs and Energy (BMWi) and the German Aerospace Center (DLR) Space Administration Agency for funding this work as well as the DLR Mobile Rocket Base (MORABA) department, the Center of Applied Space Technology and Microgravity (ZARM) and the European Space Agency (ESA) for their support.

### References

- [1] Peery DJ. Aircraft structures. Mineola, New York: Dover publications; 2011.
- [2] Breuer UP. Commercial Aircraft Composite Technology. 1st ed. Cham: Springer International Publishing; Springer; 2018.
- [3] Ageorges C, Ye L, Derby B. Fusion Bonding of Polymer Composites. London: Springer London; 2002.
- [4] Ehard S, Mader A, Ladstätter E, Drechsler K. Thermoplastic Automated Fiber Placement for Manufacturing of Metal-Composite Hybrid Parts. In: Hausmann JM, Siebert M, editors. Euro Hybrid: Materials and Structures. Kaiserslautern; 2016, p. 129–34.
- [5] Kollmannsberger A, Lichtinger R, Hohenester F, Ebel C, Drechsler K. Numerical analysis of the temperature profile during the laser-assisted automated fiber placement of CFRP tapes with thermoplastic matrix. *Journal of Thermoplastic Composite Materials* 2017;31(12):1563–86.
- [6] Sonmez FO, Hahn HT. Analysis of the On-Line Consolidation Process in Thermoplastic Composite Tape Placement. *Journal of Thermoplastic Composite Materials* 2016;10(6):543–72.
- [7] Ehrenstein GW, Theriault RP. Polymeric materials: Structure, properties, applications. Munich: Hanser; Hanser Gardner Publications; 2001.
- [8] Peters ST. Handbook of Composites. Boston, MA: Springer US; 1998.
- [9] Davis BA. Compression molding. Munich: Hanser; 2003.
- [10] Eguémann N, Giger L, Roux M, Dransfeld C, Thiébaud F, Perreux D. Compression Moulding of Complex Parts for the Aerospace with Discontinuous Novel and Recycled Thermoplastic Composite. In: Van Hoa S, Hubert P, editors. ICCM19: 19th International Conference on Composite Materials. Montreal; 2013, p. 6616–26.
- [11] Engelhardt R, Oelhafen J, Ehard S, Kollmannsberger A, Drechsler K. Manufacturing of a Thermoplastic CFRP Rocket Module with Integrated Fiber Optical Temperature Sensors. In: SICOMP29: 29th Conference on Manufacturing and Design of Composites, Lulea, Sweden, 28-29th May 2018.
- [12] Kölzer P. Temperaturerfassungssystem und Prozessregelung des laserunterstützten Wickelns und Tapelegens von endlos faserverstärkten thermoplastischen Verbundkunststoffen. Aachen: Shaker; 2008.
- [13] Ehard S. Untersuchung eines laserbasierten Ablegeverfahrens zur Herstellung von hybriden Metall-Thermoplast-Faserverbundstrukturen. München: Dr. Hut; 2019.
- [14] Schäfer PM. Consolidation of carbon fiber reinforced polyamide 6 tapes using laser-assisted tape placement. 1st ed. München: Verlag Dr. Hut; 2018.
- [15] TEIJIN. Material Data Sheet: Tenax®-E TPUD PEEK-HTS45. Wuppertal, Germany; 2018.
- [16] VICTREX. Material Data Sheet: VICTREX® PEEK 450CA30. Lancashire, United Kingdom; 2016.
- [17] ASTM D5868-01 (2014). Standard Test Method for Lap Shear Adhesion for Fiber Reinforced Plastic (FRP) Bonding. West Conshohocken, PA: ASTM International; 2014. doi:10.1520/D5868-01R14; Available from: [www.astm.org](http://www.astm.org).
- [18] Hellerich W, Harsch G, Baur E. Werkstoff-Führer Kunststoffe: Eigenschaften, Prüfungen, Kennwerte. 10th ed. München: Hanser; 2010.
- [19] Schürmann H. Konstruieren mit Faser-Kunststoff-Verbunden. 2nd ed. Berlin, Heidelberg: Springer-Verlag Berlin Heidelberg; 2007.
- [20] Mason K. A giant leap in rocket weight savings: CFRP module saves weight on rocket design: *Composites World*; 2019.
- [21] European Space Agency. REXUS 23 launched!: Space for education; 2019.